



A DFT study of ruthenium pincer carboxylate complexes as potential catalysts for the direct carboxylation of arenes with CO₂ – meridional versus facial coordination

Journal:	<i>Dalton Transactions</i>
Manuscript ID:	DT-ART-01-2014-000294.R1
Article Type:	Paper
Date Submitted by the Author:	07-Mar-2014
Complete List of Authors:	Hoelscher, Markus; RWTH Aachen University, Institute of Technical and Macromolecular Chemistry Stoychev, Spas; RWTH Aachen University, Institute of Technical and Macromolecular Chemistry Conifer, Christopher; RWTH Aachen University, Institute of Technical and Macromolecular Chemistry Uhe, Andreas; RWTH Aachen University, Institute of Technical and Macromolecular Chemistry Leitner, Walter; RWTH Aachen University, Institute of Technical and Macromolecular Chemistry



ARTICLE

A DFT study of ruthenium pincer carboxylate complexes as potential catalysts for the direct carboxylation of arenes with CO₂ – meridional versus facial coordination

Cite this: DOI: 10.1039/x0xx00000x

Received 00th January 2012,
Accepted 00th January 2012

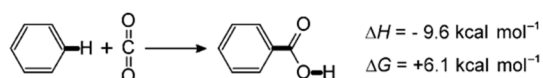
DOI: 10.1039/x0xx00000x

www.rsc.org/S. D. Stoychev^a, C. Conifer^a, A. Uhe, M. Hölscher^a*, and Walter Leitner^a

A recent DFT study of the ruthenium pincer benzoate complex [Ru(PNP)(PhCOO)₂] **I** (PNP = 2,6-bis(diphenylphosphanyl)lutidine) in its meridional form has revealed *mer-I* to be a promising catalyst lead structure for the direct insertion of CO₂ into the C-H bonds of arenes, such as benzene. After successful synthesis of **I** its solid state structure interestingly and unexpectedly showed the pincer ligand to adopt the *facial* rather than the *meridional* coordination mode. Recalculation of the catalytic cycle with *fac-I* including all relevant local minima and transition states revealed a) *fac-I* to be significantly more stable (6.1 kcal/mol) than *mer-I*, b) that the energetic span (ES; i.e. the effective activation barrier) for the cycle with *fac-I* amounts to 38.8 kcal/mol, while the cycle with *mer-I* has an ES of 25.5 kcal/mol only. These results hint at *fac-I* to be catalytically inactive. Experimental testing of *fac-I* showed indeed no product formation, which is in full accordance with the computations. To reduce the spatial flexibility of the pincer ligand its CH₂ groups were replaced by O atoms. The resulting complex [Ru(PONOP)(PhCOO)₂] **II** (PONOP = 2,6-bis(diphenylphosphinito)pyridine) was used for the calculation of the catalytic cycle in benzene as the solvent. Gratifyingly, the starting complex *mer-II* is more stable than *fac-II* by 1.9 kcal/mol in benzene as the solvent. Consequently, *mer-II* should be available experimentally. As with *fac-I* also *fac-II* generates a catalytic cycle with a high ES (37.1 kcal/mol), while *mer-II* generates a cycle with a significantly lower ES (27.2 kcal/mol) indicating *mer-II* to be a potentially active catalyst. A possible explanation of the much lower ES in the case of the meridionally coordinated species is found in the stronger interaction of the substrate with the metal center in the arene-σ-bond complex. As a result the issue that is created by the *mer/fac* isomerism can be resolved by creating spatially less flexible structures.

Introduction

The utilization of CO₂ in the chemical value creation chain is a scientific and technological challenge in many areas of chemistry due to the thermodynamic and kinetic stability of this otherwise very attractive C₁ building block.^[1,2] For instance the insertion of CO₂ into the C-H bonds of arenes would directly yield aromatic organic acids, which are interesting intermediates and end products in the commodity and fine chemical sector.^[3-5] A direct arene carboxylation, which is exemplified for benzene as the aromatic substrate in Scheme 1, would be a very attractive reaction from both academic and industrial viewpoints.^[6-8]

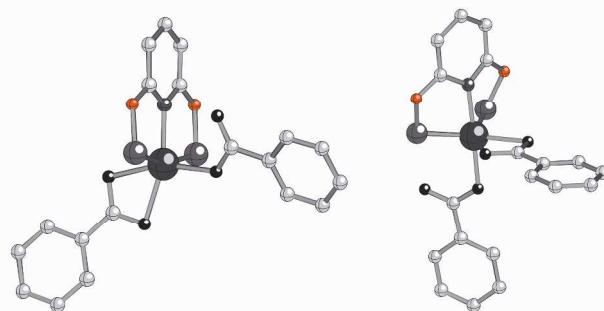


Scheme 1. Standard state thermodynamics of the hydroarylation of CO₂.

Even though the reaction of CO₂ with benzene is an exothermic process ($\Delta H = -9.6$ kcal/mol) the reaction is not feasible due to an unfavorable entropic contribution which renders the transformation endergonic ($\Delta G = +6.1$ kcal/mol).^[9] A thermodynamic driving force can be generated by introducing an appropriate base in analogy to the hydrogenation of CO₂ to formic acid.^[10] The base solves the thermodynamic challenge of this reaction and limits the scientific challenge to finding a suitable catalyst for the activation/breaking of the arene C-H bond and the C-C bond forming event between the arene and CO₂. To approach this problem we have recently developed an intuition based mechanistic scenario which was used for catalyst lead structure determination by computational screening of a large variety of ruthenium carboxylate pincer complexes with meridionally coordinating pincer ligands.^[11] It was possible to identify promising lead structures which led to the initiation of experimental work in which it was discovered that with pincer complexes the *fac/mer* isomerism can be an issue with regard to the catalytic behavior of such complexes which needs to be resolved. Here we discuss the details of this issue and propose solutions to this problem. In fact we note, that one can have the impression that DFT has predicted the “wrong” catalyst in our earlier work. However, this is not the case. Instead we were surprised by the fact that facial complexes will play a role in this system. As such this work is a nice example, that significant care needs to be taken while conducting computational catalyst development in order not to overlook alternative catalyst isomers, reaction pathways or reaction products.

In more detail, we have synthesized and characterized the bis benzoate ruthenium complex [Ru(PNP)(PhCOO)₂] **I** (PNP = 2,6-bis(diphenylphosphanyl)lutidine) of which an X-ray crystallographic characterization was possible.^[12] Interestingly, the solid state structure of **I** showed the pincer ligand to adopt a facial structure which is rather unusual for this particular ligand. Catalytic testing of *fac-I* showed it to be inactive for CO₂ insertion into arenes. As our previous calculations for *mer-I* had shown an encouragingly low ES we reasoned that the corresponding ES for *fac-I* should be much higher. Here, we report on the computations and the detailed comparison of the energy profiles of *fac-I* and *mer-I* and elucidate the reasons for the catalytic inactivity of *fac-I* in detail. From these results we extend our computational work and present an improved catalyst candidate **II**, which contains the PONOP pincer ligand

(PONOP = 2,6-bis(diphenylphosphinito)pyridine) as this ligand is expected to be structurally less flexible. The structures of compounds **I** and **II** in facial and meridional coordination mode are shown in Scheme 2, whereas the details of the catalytic cycles are discussed in detail below.



Scheme 2. Computed structures of C-H-activating ruthenium pincer complexes **I** and **II** in meridional (left) and facial (right) coordination (CH₂ and O groups in the bridge between the pyridine ring and P atoms in **I** and **II**, respectively, are shown in red). Hydrogen atoms and phenyl rings on P atoms were omitted for clarity.

Computational Details

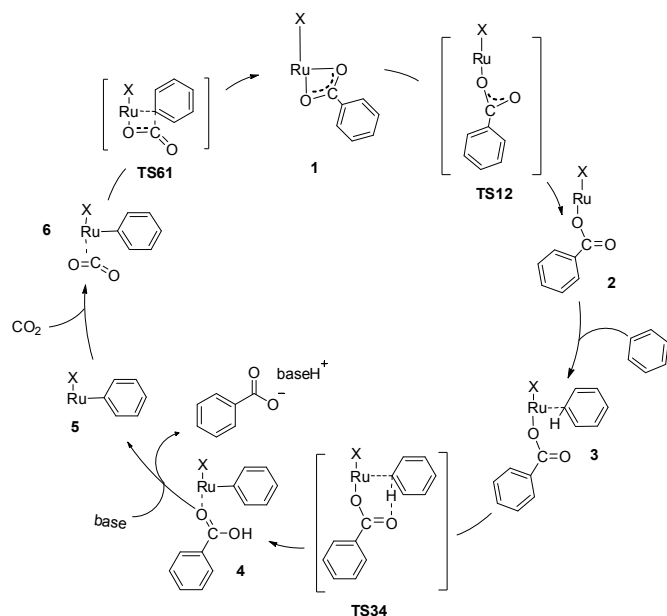
The DFT calculations in this work were carried out with the Gaussian09 program package.^[13] We used the M06-L density functional that was parameterized by taking “dispersion-like” (“medium-range”) correlation energy into account.^[14] Double and triple zeta valence basis sets with polarization functions by Weigend and Ahlrichs^[15] (termed def2-SVP and def2-TZVP) were placed on all elements together with the associated ECPs for ruthenium.^[16] The automatic density fitting approximation implemented in Gaussian 09 was also applied.^[17] The nature of all of the stationary points located were verified by frequency calculations confirming the presence of local minima ($i=0$) or transition states ($i=1$). Where necessary, the geometries of the gas phase structures were fully reoptimized in solvent phase using the polarizable continuum model (PCM).^[18] The translational entropy term of the PCM calculations was corrected as described earlier.^[19] The Gibbs free energies (ΔG) were calculated for 298.15 K and 1 atm pressure unless noted otherwise. Tables listing all of the energies obtained, as well as the Cartesian coordinates of all compounds are included in the Supporting Information (SI).

Results and Discussion

Catalytic cycle for the PNP complex series

Ruthenium pincer complexes were chosen previously as the starting points for a potential catalytic cycle mainly for three reasons.^[11] 1: Molecular catalysts of the late transition metals and especially pincer complexes have proven as efficient catalysts for C-H bond activation and transformation for both arene and alkane substrates.^[20,21] 2: Ruthenium pincer complexes are known to bind and activate CO₂.^[2d-f,h-j, 10, 21b-d,] 3: Experimental studies in our group have shown ruthenium pincer complexes to be active catalysts in the activation of arene C-H bonds.^[22]

A plausible catalytic cycle is shown in Scheme 3 and exemplifies the reaction for benzene as the aromatic substrate. The reasoning for this mechanistic scenario was as follows: If the desired catalytic event (i.e. the formation of the C-C bond between CO₂ and an arene) does occur, then it is likely that the initial reaction product –namely a benzoate moiety– is present at the catalyst at some stage of the reaction.



Scheme 3. Prototypical mechanism for direct carboxylation of benzene with CO₂ (Ru = ruthenium pincer fragment, see Scheme 2; X = monodentate, anionic ligand). For clarity the pincer ligand is omitted.

If one assumes the catalyst to be a neutral octahedrally coordinated ruthenium(II) pincer complex with a neutral pincer ligand, three coordination sites will be occupied in meridional coordination mode by this ligand. Two of the remaining three coordination sites will be occupied by the oxygen atoms of the monoanionic benzoate unit and the remaining coordination site will be occupied by a monodentate ligand X (a halogen ion, a monocoordinated benzoate anion, etc.) yielding an overall electroneutral complex. Accordingly, one arrives at structure **1** as the catalytically active starting species of the cycle (Scheme 3). Regarding a discussion of the single steps of the cycle we refer the reader to ref.^[11] for detailed information. In the present work though, the catalytic cycle is extended by the transition state for the decoordination of the ligand participator (TS1-2). As a result of our initial computational work we identified a variety of meridionally coordinated ruthenium benzoate pincer complexes potentially active for the direct carboxylation of arenes

with CO₂. To elucidate and verify the computationally predicted reactivity, complex **I** was synthesized. A single crystal X-ray diffraction study of **I** revealed interestingly, that **I** in the solid state is not present as the expected meridionally coordinated compound *mer-I*, instead the complex is coordinated facially by the pincer ligand (*fac-I*).^[12] Although facial pincer ligation has been observed it is relatively unusual. The presence of *fac-I* led us to the conclusion that the energy of the starting complex **I-1** and the complete catalytic cycle needs to be recalculated for the *fac*-series of isomers. It was possible to reoptimize all intermediates and transition states in the *fac*-form. The energy profiles calculated for *fac-I* and *mer-I* are shown in Figure 1. Table 1 summarizes the relative energies together with the calculated energetic span. At first the results for our gas-phase computations with the more modest def2-SVP basis set are discussed to draw the qualitative picture of the investigated systems. A detailed discussion of the single reaction steps is given in the SI. Here, we focus on the core results. We note that at steps *fac-I-1*, *fac-I-3* and *fac-I-5* an isomerization to the corresponding *mer*-isomers could occur. Therefore, such an isomerization process was located computationally and is described in full detail in section S3 of the SI. Even though isomerization can take place at several stages of the catalytic cycle, the conclusions which will be made below do not change. In other words: Isomerization will not lead to a lower energetic span for complexes with the PNP ligand (**I-series**), and also it will not change the span for the complexes with the PONOP ligand (**II**).

As can be seen from Figure 1, the facially coordinated compound is more stable than the meridionally coordinated one by 6.1 kcal/mol. This is a pronounced stability difference which explains the experimentally observed formation of *fac-I* instead of *mer-I*. Furthermore, the comparison of the two energy profiles shows the ES for the *fac*-profile to be much larger (38.8 kcal/mol) than the one for the *mer*-profile (25.5 kcal/mol). This is a strong hint that in contrast to the predictions made earlier for *mer-I*, *fac-I* might not lead to productive catalytic turn overs for the insertion of CO₂ into the C-H bond of benzene even at elevated temperatures. As a rough estimation an activation

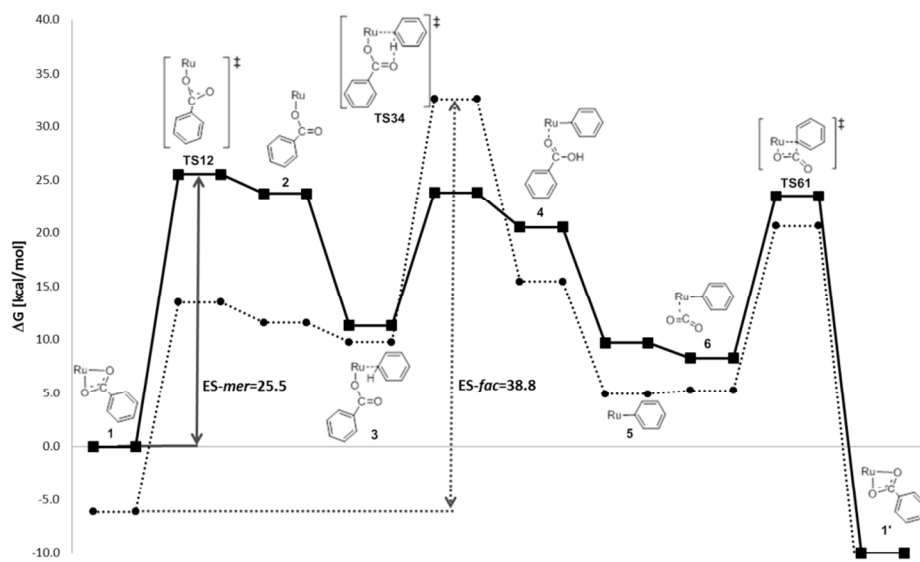


Figure 1. Gibbs free energy profiles (M06-L / def2-SVP(ECP)) for the catalytic cycle outlined in Scheme 3 for catalysts *fac-I* (dotted line) and *mer-I* (solid line), see also Table 1. In the structures the pincer ligand was omitted for clarity.

barrier of 38.8 kcal/mol would result in a rate constant k of ca. 0.043 h^{-1} at a reaction temperature of 200°C , which resembles one turn over per day.^[25]

In accordance with the computational indications an extensive catalytic testing of **I** under various reaction conditions showed it to be inactive for the insertion of CO_2 into benzene and other arenes. Therefore we assign this inactivity to the fact that *fac*-**I** while showing a closed catalytic cycle has a too large ES for the reaction to proceed.

(see SI). This in turn should decrease the preference for facial coordination and make meridional coordination competitive or even preferred.

Table 1. Relative Gibbs free energies of all stationary points of the catalytic cycle and energetic spans (ESs) both in kcal/mol.^[a]

Complex	Stationary points and transition states									ES	Basis set
	1	TS1-2	2	3	TS3-4	4	5	6	TS6-1'		
PNP											
Meridional	0.0	25.5	23.7	11.3	23.8	20.5	9.7	8.3	23.5	25.5	def2-SVP
Facial	-6.1	13.5	11.6	9.8	32.6	15.5	4.9	5.3	20.6	38.8	def2-SVP
PONOP											
Meridional	0.0	26.3	22.7	12.0	23.3	18.9	9.7	6.6	22.3	26.3	def2-SVP
Facial	0.1	19.5	18.0	14.5	31.9	25.7	8.3	6.4	25.5	31.8	def2-SVP
Meridional ^[b]	0.0	25.4	21.2	11.0	24.8	20.9	7.8	4.6	22.5	25.4	def2-TZVP
Meridional ^[b,c]	0.0	25.9	21.2	13.0	27.2	23.1	5.7	4.0	23.0	27.2	def2-TZVP

^[a]M06-L; 1,8-bis(diethylamino)-2,7-dimethoxynaphthalene (BDN) was used as the base; see also Ref. [11].

^[b]Benzene included as solvent with the PCM model.

^[c]Calculated values for $T = 373 \text{ K}$, all other values were computed for $T = 298.15 \text{ K}$.

Catalytic cycle for the PONOP complex series

In order to modify the catalyst structure we reasoned that the replacement of the CH_2 groups in the pincer ligand by O atoms should lead to a more rigid structure, because the unpaired electrons of the O atoms can contribute to resonance effects with the aromatic pyridine system via partial C-O double bond formation between the pyridine moiety and the bridging oxygen atom. In this way the rigidity of the ligand should be increased

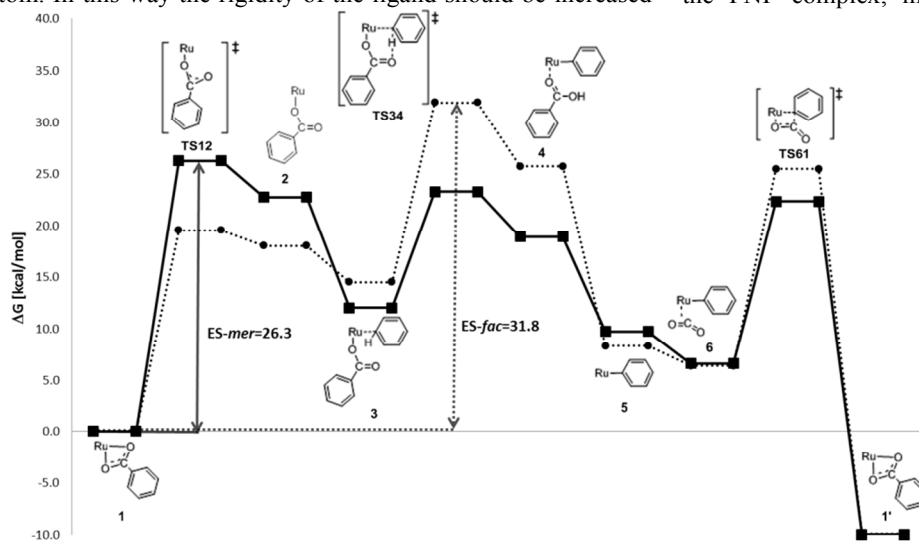


Figure 2. Gibbs free energy profiles (M06-L / def2-SVP(ECP)) for the catalytic cycle outlined in Scheme 3 for catalysts *fac*-**II** (dotted line) and *mer*-**II** (solid line), see also Table 1. In the structures the pincer ligand was omitted for clarity.

The free energy profiles of the catalyst system with the PONOP ligand in facial and meridional coordination are depicted in Figure 2. Gratifyingly, the meridional and the facial coordination mode have practically the same stability ($\Delta G = 0.1 \text{ kcal/mol}$ in favor of *mer*-**II**; more accurate calculations including solvent effects are described in a later section). Also for this cycle the starting structure (**II-1**) is the TDI for both coordination modes, while *fac*-**II**-(TS3-4) and *mer*-**II**-(TS1-2) are the TOF determining transition states.

The energy of *mer*-**II**-(TS1-2) is 26.3 kcal/mol, showing that the decoordination of the benzene molecule is, in analogy with the PNP complex, much easier in the facially coordinated

species where *fac*-**II**-(TS1-2) is by 6.8 kcal/mol more stable. The other transition states of the meridionally coordinated system are below *mer*-**II**-(TS1-2) by two to three kcal/mol. This is an encouraging indication with regard to a potential experimental application. Instead, the TDTS computed for the facially coordinated complex series *fac*-**II**-(TS3-4) resides much higher on the hyper surface (31.8 kcal/mol).

Next we extended the computational catalyst screening for **II** to the calculation of complete catalytic cycles with broadly varied catalyst systems. These variations include the use of different

spectator ligands, different substrates and various solvents. The results are summarized in Table S1 and S2 of the SI and they imply that in all of the studied complexes the meridional coordinated complex series is the preferred one with regard to a catalytic application. It turned out that **II** (i.e. the catalyst system with benzoate anions as participator/spectator ligands and benzene as reactant including benzene as the solvent) is the most interesting one with regard to a potential catalytic application. Therefore, this system is investigated in more detail and in comparison with **I** in the following sections.

Bonding analysis of **I** and **II**

Considering that the coordination mode of the initial state of the catalytic cycle will determine if the species is catalytically active, **I-1** and **II-1** were investigated in more detail. The stability of the *fac*- and *mer*- isomers is related to the interaction of the ruthenium center with the ligands. This interaction can be divided into the bonding energy and the deformation energy of the ligands. The latter is the difference between the Gibbs free energies of the molecular fragments (the pincer and the two benzoate anions) with their geometries in the complex and the Gibbs free

energies of the same structures optimized as isolated molecules (Table 2). In their relaxed geometries, the P atoms of both the PNP and the PONOP ligand are located only slightly out of the plane defined by

the pyridine rings. Thus, the geometries of the free pincer ligands resemble more the structure they adopt in the meridional than in the facial complexes. The more flexible CH₂ groups connecting the P atom with the aromatic ring in the PNP system make the deformation energy of *fac*-**I-1** (21.6 kcal/mol) similar to that of *mer*-**I-1** (18.3 kcal/mol) leading to an energy difference of only 3.3 kcal/mol. In contrast in the PONOP containing system, the energy difference of the two isomers is much larger (7.4 kcal/mol) with the deformation energy of *fac*-**II-1** being a little higher (22.9 kcal/mol) than *fac*-**I-1** and *mer*-**II-1** (15.5 kcal/mol) being a little smaller than *mer*-**I-1**. This proves that the substitution of the bridging CH₂ group in the pincer ligand with an O atom has led to a more rigid structure, as significantly more energy is used for deformation.

As the deformation energies of the benzoate ions are very similar in both the PNP and the PONOP systems, the total deformation energies (column 5 in Table 2) are determined by considering the deformation energy of the pincer molecules only. The total deformation energy in *fac*-**I-1** (29.9 kcal/mol) differs from that of *mer*-**I-1** by 2.0 kcal/mol. This is only a small difference indicating that the energetic effort that must be made to deform the ligands from their relaxed geometries to the ones they adopt in the PNP complexes is very similar. In contrast, the total deformation energy in the PONOP containing complex is 31.6 kcal/mol in the facial and 25.3 kcal/mol in the meridional isomer. This indicates that significantly more energy is needed to deform the ligands in *fac*-**II-1**.

The deformation energy alone, favors the formation of the *mer*-isomer in both structures **I-1** and **II-1**, especially in the PONOP case where the difference of the deformation energies in the two isomers is more than seven kcal/mol. However, the *mer*-**I-1** isomer is less stable than the *fac*-**I-1** and *mer*-**II-1** just slightly more stable than *fac*-**II-1**.

Table 2. Deformation energies of the ligands (kcal/mol) computed as the difference of the ΔG of the complex fragments and their optimized geometries.^[a]

Compound	Pincer	Benzoate		Total
		participator	spectator	
<i>fac</i> - I-1	21.6	5.6	2.7	29.9
<i>mer</i> - I-1	18.3	6.7	2.9	27.9
<i>fac</i> - II-1	22.9	6.0	2.8	31.6
<i>mer</i> - II-1	15.5	6.8	3.0	25.3

^[a]M06-L / def2-SVP(ECP)

Thus, the bonding of the metal center to the ligands needs to be considered in order to clarify the stability of the PNP and PONOP containing complexes (Table 3). The relative bonding energies ΔG^{rel}_{bond} are derived as shown in eq. (1) – (3) (*fac*-**I-1** is chosen as the reference point).

$$\Delta G^{rel}_{bond} = \Delta G^{mer-I-1}_{bond} - \Delta G^{fac-I-1}_{bond} \quad (1)$$

$$\Delta G^{mer-I-1}_{bond} = \Delta G^{mer-I-1} - (\Delta G^{Ru2+} + \Delta G^{mer-I-1}_{PNP} + \Delta G^{mer-I-1}_{Benz.S} + \Delta G^{mer-I-1}_{Benz.P}) \quad (2)$$

$$\Delta G^{fac-I-1}_{bond} = \Delta G^{fac-I-1} - (\Delta G^{Ru2+} + \Delta G^{fac-I-1}_{PNP} + \Delta G^{fac-I-1}_{Benz.S} + \Delta G^{fac-I-1}_{Benz.P}) \quad (3)$$

In equation (2) $\Delta G^{mer-I-1}_{bond}$ is the bonding energy of the ligands with the metal center in *mer*-**I-1**. There, $\Delta G^{mer-I-1}$ is the Gibbs free energy of *mer*-**I-1** and ΔG^{Ru2+} , $\Delta G^{mer-I-1}_{PNP}$, $\Delta G^{mer-I-1}_{Benz.S}$, and $\Delta G^{mer-I-1}_{Benz.P}$ are the Gibbs free energies of the fragments that build it. In analogy, in equation (3) $\Delta G^{fac-I-1}$ is the Gibbs free energy of *fac*-**II-1** and ΔG^{Ru2+} , $\Delta G^{fac-I-1}_{PNP}$, $\Delta G^{fac-I-1}_{Benz.S}$, and $\Delta G^{fac-I-1}_{Benz.P}$ are the Gibbs free energies of the fragments that build it. Note that when computing ΔG^{rel}_{bond} in this fashion, the Gibbs free energies of the metal ions cancels out and therefore are not needed to compute the bonding energies.

With the bonding energies and the deformation energies for each complex the relative stabilities can be computed. For the PNP containing system it was already shown above that the deformation energy of the *mer*- isomer is by 2.0 kcal/mol lower than that of the *fac*- isomer. The bonding energy in *fac*-**I-1** is by 8.1 kcal/mol stronger than in *mer*-**I-1**. When the deformation energy and the bonding energy is summed up, it results that *fac*-**I-1** is by 6.1 kcal/mol more stable than *mer*-**I-1**, which is exactly the value computed directly and independently (Table 1). In the PONOP containing system, the difference in the bonding energies of *fac*-**II-1** and *mer*-**II-1** is 6.2 kcal/mol in favor of the complex containing the facially coordinated species. Adding the deformation energy (6.3 kcal/mol higher in the facial case) to the bonding energy it turns out that the meridionally coordinated system is by 0.1 kcal/mol more stable, again matching the value that was computed directly.

The bonding energies which we have just discussed show that in the *fac*-PNP containing system the bonding of the metal center with the ligand is strong. This makes it the more stable isomer although the deformation energy there is larger than in *mer*-**I-1**. In the case of the PONOP complex, the differences in the deformation and the bonding energies of the *fac*- and *mer*-isomers cancel each other and make the two isomers very close in energy.

Table 3. Relative Gibbs free bonding energies (kcal/mol) of the studied complexes relative to *fac-I-1*.^[a]

Compound	Relative $\Delta G_{\text{bond}}^{\text{rel}}$ of bonding
<i>fac-I-1</i>	0.0
<i>mer-I-1</i>	8.1
<i>fac-II-1</i>	5.7
<i>mer-II-1</i>	11.9

^[a]M06-L / def2-SVP(ECP)

Subsequently, the bonding energy of the pincer ligand to the metal center only is investigated. For this purpose, we shall again use the single point energies of the fragments with geometries identical to the ones in the complex. At first the relative energies of the bonding between the pincer and the Ru²⁺ ion ($\Delta G_{\text{bond [Ru-pincer]}2+}^{\text{rel}}$), shown in Table 4 is inspected. The species containing the PNP molecule in facial coordination mode is used as a reference point, since the pincer–Ru²⁺ bonding interaction is the strongest for this molecule. It is 37.1 kcal/mol stronger than the bond between the ruthenium ion and the PNP molecule in meridional coordination mode. This

$$\Delta G_{\text{bond [Ru-pincer]}2+}^{\text{rel}} = \Delta G_{\text{bond[Ru-PNP]}2+}^{\text{mer-I-I}} - \Delta G_{\text{bond[Ru-PNP]}2+}^{\text{fac-I-I}} \quad (4),$$

$$\Delta G_{\text{bond[Ru-PNP]}2+}^{\text{mer-I-I}} = \Delta G_{\text{[Ru-PNP]}2+}^{\text{mer-I-I}} - (\Delta G^{\text{Ru}2+} + \Delta G_{\text{PNP}}^{\text{mer-I-I}}) \quad (5),$$

$$\Delta G_{\text{bond[Ru-PNP]}2+}^{\text{fac-I-I}} = \Delta G_{\text{[Ru-PNP]}2+}^{\text{fac-I-I}} - (\Delta G^{\text{Ru}2+} + \Delta G_{\text{PNP}}^{\text{fac-I-I}}) \quad (6),$$

energy difference is obtained using eq. (4)-(6):

$\Delta G_{\text{bond[Ru-PNP]}2+}^{\text{mer-I-I}}$ is the bonding energy of the pincer in meridional coordination mode with the ruthenium ion. There, $\Delta G_{\text{[Ru-PNP]}2+}^{\text{mer-I-I}}$ is the Gibbs free energy of [Ru-PNP *mer-I-I*]²⁺ and $\Delta G^{\text{Ru}2+}$ and $\Delta G_{\text{PNP}}^{\text{mer-I-I}}$ are the Gibbs free energies of the fragments that build it.

In equation 6: $\Delta G_{\text{[Ru-PNP]}2+}^{\text{fac-I-I}}$ is the Gibbs free energy of [Ru-PNP *fac-I-I*]²⁺, while $\Delta G^{\text{Ru}2+}$ and $\Delta G_{\text{PNP}}^{\text{fac-I-I}}$ are the Gibbs free energies of the fragments that build it.

Remarkably, the computed results suggest that in both the PNP and the PONOP systems the bonding of the pincer ligand in the facially coordinated species is much better than in the meridionally coordinated ones. In fact, this is the reason for the better stability of *fac-I-1* in comparison to *mer-I-1*. In the case of the PONOP bonded to Ru²⁺, the energy difference between the meridionally and facially coordinated species is also large (27.8 kcal/mol). Accordingly, an untypical stability for the Ru pincer complexes of the systems is observed in which the pincer molecule is considerably deformed.

The bonding energies of the complexes containing meridionally and facially coordinated species differ more in the [Ru-pincer]²⁺ species than in the complete catalyst complexes *I-1* and *II-1* that contain them. Thus, the bonding of the metal center with the benzoate anions should be stronger in the case of the meridionally coordinated species as is clearly shown in Table 5. The bonding energy of the two benzoate anions is the highest one in *mer-II-1* (381.8 kcal/mol). Note that the table

also contains the energies of the bonding of single benzoate anions to the studied ruthenium-pincer complexes.

Table 4. Relative Gibbs free energies (kcal/mol) of [Ru-pincer]²⁺ complexes with geometries taken from *I-1* and *II-1*.^[a]

Geometry of Ru-pincer from:	$\Delta G_{\text{[Ru-pincer]}2+}^{\text{rel}}$
<i>fac-I-1</i>	0.0
<i>mer-I-1</i>	37.1
<i>fac-II-1</i>	22.9
<i>mer-II-1</i>	50.7

^[a]M06-L / def2-SVP(ECP)

Our results for the bonding energies of the ligands in the system are also supported by a computation of the natural bond orbital (NBO) charges of the pincers and the Ru-pincer fragments of the complex. The substitution of the bridging –CH₂– groups in the PNP systems with O atoms has not only made the structure more rigid leading to larger deformation energies, but it has also changed the charge at atoms that bond to the metal center. The partial positive charge at the P atoms in the PNP systems is 0.86-0.87 a.u. while in the PONOP containing ones it is 1.1-1.4 a.u.. Consequently, the electrostatic repulsion between the positively charged ruthenium ion and the pincer atoms that attach to it is greater in the latter case. The weaker bonding of the pincer to the metal ion in the meridional case also leads to a higher positive partial charge at Ru (0.5 a.u. in *mer-I-1* and 0.4 a.u. in *mer-II-1*) in comparison to *fac-I-1* and *fac-II-1* (0.1 a.u.). This makes the electrostatic attraction between the metal center and the benzoate anions that attach later stronger in the meridionally coordinated species and leads to a stronger bond.

Table 5. Gibbs free energies of bonding of the benzoate anions (kcal/mol).^[a]

Geometry from:	Bonding energy of:				
	Participator and Spectator	Participator (spectator attached)	Spectator (participator attached)	Participator (spectator missing)	Spectator (participator missing)
<i>fac-I-1</i>	343.0	137.4	121.5	221.5	205.6
<i>mer-I-1</i>	371.9	146.0	124.4	247.6	226.0
<i>fac-II-1</i>	360.2	142.5	130.5	229.7	217.7
<i>mer-II-1</i>	381.8	153.4	129.5	252.2	228.4

^[a]M06-L / def2-SVP(ECP)

Quantitative explanations

In order to make a quantitative evaluation of the properties of the investigated systems and get more accurate values for the ES and TOF of catalytic cycle we have resorted to a better quality computation for the experimentally most feasible system. Using the def2-TZVP basis set and introducing benzene as solvent with the PCM model. We first optimized the geometries of *II-1* and found that *mer-II-1* is indeed more stable than *fac-II-1* by 1.9 kcal/mol. However, as the energy difference is relatively small one would expect upon synthesizing *II* both isomers to be experimentally available.

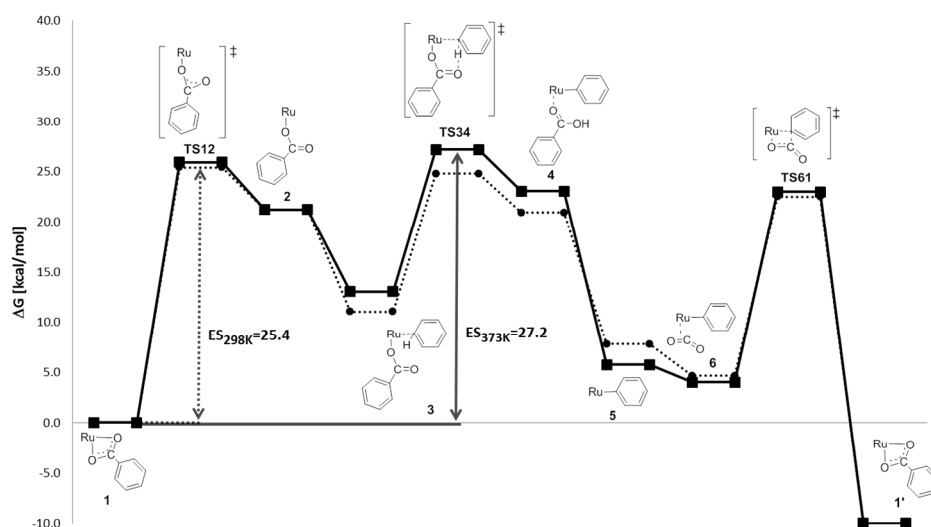


Figure 3. Gibbs free energy profiles (M06-L / def2-TZVP(ECP) / benzene (PCM)) for the catalytic cycle outlined in Scheme 3 for catalyst *mer-II* at 298.15 K (dotted line) and 373 K (solid line), see also Table 1. In the structures the pincer ligand was omitted for clarity.

We continued with reoptimizing the geometries and recomputed the energies of all of the intermediates and transition states of the PONOP system in meridional coordination mode. The resulting free energy profiles for the temperatures of 298.15 K and 373 K are shown in Figure 3. The two curves almost overlap in states **II-1** to **II-2**, while the transition state for the decoordination of the benzoate participator anion (**TS1-2** at 25.4 kcal/mol) is the highest effective activation barrier computed for 298.15 K. However, the energy of **TS1-2** at the lower temperature does not differ much from that of the other transition states, being slightly higher than **TS3-4** and about 3 kcal/mol higher than of **TS6-1** (the C-C bond formation). These ΔG differences are very close to the results obtained for 298.15 K with the smaller basis in gas phase as already discussed.

The coordination of the benzene molecule in **II-3** leads to a decrease of the free energy. Here, however, the entropic component of ΔG is expectedly influenced by the temperature. Thus, the free energy of **II-3** at 373 K is 2.0 kcal/mol higher than that at 298.15 K.

In comparison, the difference in the increase of ΔH for the two temperatures is only 0.1 kcal/mol. The shift in ΔG with the temperature is also valid for **II-TS3-4** and makes it the TDTS at 373 K with its 27.2 kcal/mol above the TDI (**II-1**). With the more precise value of the ES obtained for the elevated temperature a TOF of 3.3 h^{-1} was computed using the energetic span model developed by Kozuch and Shaik.^[25]

The energy barrier for the C-C bond formation (**TS6-1**) increases slightly (from 22.5 to 23.0 kcal/mol) with the temperature. More importantly, it is 4.2 kcal/mol below the TDTS at 373 K, which means that a weaker base than BDN ($\text{p}K_{\text{B}} = -2.1$) can be used to stabilize the product of the catalytic reaction. The energies of compounds **II-5** to **II-1'** could be allowed to rise up to the mentioned 4.2 kcal/mol and this will not change the ES. Our estimates show that any base with $\text{p}K_{\text{B}}=1$ or less will be strong enough for the reaction to take place. Thus, although a comparatively high temperature is needed for the reaction, a weaker base can be used in order to reduce the probability of catalyst degradation by the base.

Other intermediates and transition states of interest

For the sake of completeness we have recomputed the TDI and TDTS of the PONOP system in facial coordination at 373 K and in the presence of benzene as solvent to obtain the ES for the facial series of complexes for comparison. The ES amounts to 37.1 kcal/mol. It is almost 10 kcal/mol higher than the ES of the meridionally coordinated system and suggests that the *fac*-isomer will not be an active catalyst at this temperature.

In our discussion of the PONOP containing *mer*-isomer, we have considered decoordination of the benzoate participator ligand that generates a vacant coordination site opposite to the N atom of the pincer (Scheme 3). However, the

benzoate can decoordinate with the other O, creating a vacant coordination site opposite to the spectator ligand. This alternative reaction pathway creates a system in which the participator ligand and the substrate have changed their places. In this case, the C-H activation and the C-C bond formation that follow have to pass transition states with comparatively higher energies, 31.5 and 27.3 kcal/mol, respectively. Therefore, a much higher energetic span is observed, due to the altered environment of the metal center. Possibly, the alternative decoordination and arrangement of the ligands in the complex can be the preferred catalytic path for systems with a different backbone of the pincer ligand.

The C-H activation step

The different heights of the C-H activation barrier (**TS3-4**) in *fac-II* and *mer-II* can be explained with the structural and electronic properties of the systems. For this purpose, we shall consider the geometries of the intermediate (**II-3**) that undergoes σ -bond metathesis (Figure 4).

In the facially coordinated system, the substrate and the participator ligand position themselves at the metal center with little spatial restraints. This, however, leads to the coordination of the benzene molecule with one of its C=C bonds at a comparatively long distance from the metal center (Ru-C: 2.908 Å and 2.956 Å). In contrast, in *mer-II-3*, the substrate coordinates to the Ru atom with the C-H bond that will be cleaved in the subsequent step (Figure 4, left). This coordination mode is most likely a result of too small a space to coordinate the benzene molecule via one of its C=C bonds. Repeated attempts to localize an isomer with the C=C bond of benzene coordinated to *mer-II-3* were unsuccessful. Accordingly the the σ -C-H-bond interacting with the catalytic center in *mer-II-3* is lengthened to 1.110 Å (1.082 Å in an isolated benzene molecule). The increase of the bond length is not very pronounced, but it should facilitate the metathesis, thus lowering the energy barrier that has to be passed (*mer-II-TS3-4*).

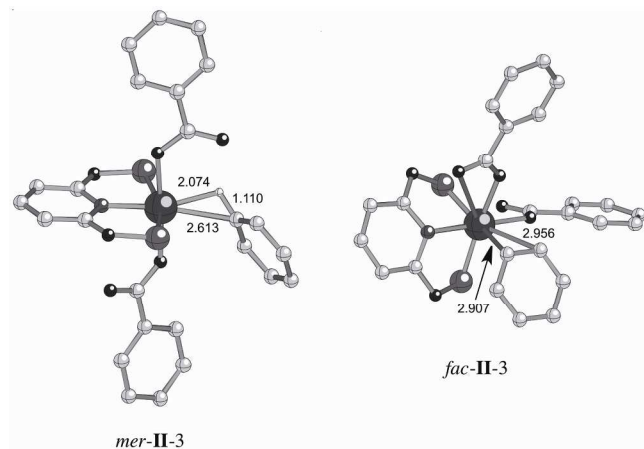


Figure 4. Ball and stick representation of *mer-II-3* (left) and *fac-II-3* (right; selected atom distances are given in Å). The structures are fully optimized with the M06-L functional and the def2-TZVP basis set in benzene as solvent. Note that in *mer-II-3* the substrate (benzene molecule) coordinates to the metal center with the C-H bond that is cleaved in a subsequent reaction step, while in *fac-II-3* the substrate coordinates with a C-C bond of the benzene ring. Phenyl groups on P atoms were omitted for clarity.

Conclusions

In this work the structural and electronic characteristics of a potentially active catalysts for the direct insertion of CO₂ into the C-H bonds of arenes were compared. Meridionally coordinating ruthenium PNP and PONOP pincer complexes *mer-I* and *mer-II*, respectively, were shown to take part in a catalytic cycle with energetic spans suggesting the reaction to take place at elevated, but reasonable temperatures. The results obtained explain in accordance with experimental work a) the formation of *fac-I* instead of *mer-I* and b) the inactivity of *fac-I* in catalytic tests. The decoordination step (TS1-2) is close in energy to the TDTS of the reaction when the *mer*-isomer of the catalyst is used. Therefore, it should not be ignored when systems of that type are studied. In the facially coordinated species, however, the situation is different and this step of the cycle can be passed easily. Nevertheless, the energetic span there is much higher due to the significantly higher energy barrier of the σ -bond-metathesis-type C-H-transfer. This explains the observed lack of catalytic activity of the PNP containing complex which is more stable in its facial coordination, as observed in the experiment.^[22] As an interconversion of *fac-I* into *mer-I* under catalytic conditions seems not possible the ligand backbone was modified. The energy profile of the catalytic cycle was recomputed for catalyst **II** containing the PONOP ligand. For **II** the meridionally coordinating complex turned out to be more stable than the facial one in all of the studied species. Our screening for catalysts included modification of the spectator and participator ligands, as well as of the substrate benzene with anisole. Remarkably, in all of the systems in meridional coordination mode the catalysis is feasible, as the computed energetic spans have similar values.

The catalytic cycle was recomputed for the experimentally most feasible system with the better quality def2-TZVP basis set and including benzene as solvent with the PCM model. This

confirmed the qualitative results of the catalyst screening and suggested that judging from the obtained ES the *mer*-isomer should be able to catalyze the carboxylation of benzene at 373 K. It was also shown that a base with a pK_B value smaller than 1 will be strong enough to stabilize the product of the reaction. Furthermore, the quantitative study of the process revealed that the C-H activation will be the TOF determining step of the cycle in both the facially and meridionally coordinated complexes. The significant difference in the energetic spans of the cycles containing *fac*- and *mer*-isomer could be explained to a certain extent by the interaction of the C-H bond being cleaved with the metal center in complex **II-3**.

Acknowledgements

This work was supported by the Deutsche Forschungsgemeinschaft (DFG) within the International Research Training Group 1628 "Selectivity in Chemo- and Biocatalysis". Computing time granted by the JARA-HPC Vergabegremium and provided on the JARA-HPC partition's part of the RWTH Bull Cluster in Aachen is gratefully acknowledged.

Notes and references

^a *Dr. S. D. Stoychev, Dr. C. Conifer, Dr. A. Uhe, Dr. M. Hölscher, Prof. Dr. W. Leitner, Institut für Technische und Makromolekulare Chemie, RWTH Aachen University, Worringerweg 1, 52074 Aachen (Germany)
Fax: (+ 49) 241-8022177

E-mail: hoelscher@itmc.rwth-aachen.de

JARA – High-Performance Computing, Schinkelstraße 2, D – 52062 Aachen

Electronic Supplementary Information (ESI) available: [details of any supplementary information available should be included here]. See DOI: 10.1039/b000000x/

- [1] a) A. Behr, *Carbon Dioxide Activation by Metal Complexes*, VCH, Weinheim, 1988; b) W. Leitner, E. Dinjus, F. Gassner in *Aqueous-Phase Organometallic Catalysis* (Eds.: B. Cornils, W. A. Herrmann), Wiley-VCH, Weinheim, 1998, pp. 486–498; c) *Catalysis by Metal Complexes, Catalysis in CI Chemistry* (Ed.: W. Keim), Reidel, Dordrecht, Boston, Lancaster, 1985; d) *Carbon Dioxide as Chemical Feedstock* (Ed.: M. Aresta), Wiley-VCH, Weinheim, 2010; e) M. Aresta, A. Dibenedetto, A. Angelini, *Chem. Rev.* 2013, DOI: 10.1021/cr4002758
- [2] a) D. Walther, *Coord. Chem. Rev.* 1987, **79**, 135 – 174; b) P. Braunstein, D. Matt, D. Nobel, *Chem. Rev.*, 1988, **88**, 747 –764; c) D. Gibson, *Chem. Rev.*, 1996, **96**, 2063 – 2095; d) W. Leitner, *Coord. Chem. Rev.*, 1996, **153**, 257 –284; e) P. G. Jessop, T. Kkariya, R. Noyori, *Chem. Rev.*, 1995, **95**, 259-272; f) P. G. Jessop, *Stud. Surf. Sci. Catal.*, 2004, **153**, 355-362; g) T. Sakakura, J.-C. Choi, H. Yasuda, *Chem. Rev.*, 2007, **107**, 2365 –2387; h) M. Aresta, A. Dibenedetto, *Dalton Trans.*, 2007, 2975 –2992; i) A. J. Morris, G. J. Meyer, E. Fujita, *Acc. Chem. Res.*, 2009, **42**, 1983 –1994; j) S. N. Riduan, Y. Zhang, *Dalton Trans.*, 2010, **39**, 3347 –3357; k) D. J. Darensbourg, *Inorg. Chem.*, 2010, **49**, 10765 – 10780; l) K. Huang, C.-L. Sun, Z.-J. Shi, *Chem. Soc. Rev.*, 2011, **40**, 2435 – 2452; m) M. Cokoja, C. Bruckmeier, B. Rieger, W. A. Herrmann, F. E. Kühn, *Angew. Chem. Int. Ed.*, 2011, **50**, 8510 –8537; n) M.

- Peters, B. Köhler, W. Kuckshinrichs, W. Leitner, P. Markewitz, T. E. Müller, *ChemSusChem*, 2011, **4**, 1216–1240.
- [3] a) G. A. Olah, A. Torok, J. P. Joschek, I. Bucsi, P. M. Esteves, G. Rasul, G. K. S. Prakash, *J. Am. Chem. Soc.*, 2002, **124**, 11379–11391; b) S. P. Bew, in *Comprehensive Organic Functional Groups Transformation II* (Eds.: A. R. Katritzky, R. J. K. Taylor), Elsevier, Oxford, 2005, pp. 19–47, c) Y. Iwasaki, K. Kino, H. Nishide, K. Kirimura, *Biotechnol. Lett.*, 2007, **29**, 819–822.
- [4] a) H. Kolbe, *Ann. Chem. Pharm.*, 1860, **113**, 125–127; b) A. Behr, *Chem. Ing. Tech.*, 1985, **57**, 893–903.
- [5] a) A. G. Myers, D. Tanaka, M. R. Mannion, *J. Am. Chem. Soc.*, 2002, **124**, 11250–11251; b) P. Forgione, M.-C. Brochu, M. St-Onge, K. H. Thesen, M. D. Bailey, F. Bilodeau, *J. Am. Chem. Soc.*, 2006, **128**, 11350–11351; c) L. J. Goossen, G. Deng, L. M. Levy, *Science*, 2006, **313**, 662–664; d) O. Baudoin, *Angew. Chem.*, 2007, **119**, 1395–1397; *Angew. Chem. Int. Ed.*, 2007, **46**, 1373–1375; e) L. J. Goossen, N. Rodriguez, K. Goossen, *Angew. Chem.*, 2008, **120**, 3144–3164; *Angew. Chem. Int. Ed.*, 2008, **47**, 3100–3120.
- [6] a) I. I. F. Boogaerts, S. P. Nolan, *J. Am. Chem. Soc.*, 2010, **132**, 8858–8859; b) I. I. F. Boogaerts, G. C. Fortman, M. R. L. Furst, C. S. J. Cazin, S. P. Nolan, *Angew. Chem.*, 2010, **122**, 8856–8859; *Angew. Chem. Int. Ed.*, 2010, **49**, 8674–8677; c) I. I. F. Boogaerts, S. P. Nolan, *Chem. Commun.*, 2011, **47**, 3021–3024.
- [7] L. Zhang, J. Cheng, T. Ohishi, Z. Hou, *Angew. Chem.*, 2010, **122**, 8852–8855; *Angew. Chem. Int. Ed.*, 2010, **49**, 8670–8673.
- [8] H. Mizuno, J. Takaya, N. Iwasawa, *J. Am. Chem. Soc.*, 2011, **133**, 1251–1253.
- [9] a) *CRC Handbook of Chemistry and Physics*, 90th ed. (Ed.: D. R. Lide), Taylor & Francis, Oxford, 2009; b) *National Institute of Standards and Technology (NIST)*: <http://webbook.nist.gov/> and the references therein.
- [10] a) F. Hutschka, A. Dedieu, W. Leitner, *Angew. Chem.*, 1995, **107**, 1905–1908; *Angew. Chem. Int. Ed. Engl.*, 1995, **34**, 1742–1745; b) F. Hutschka, A. Dedieu, M. Eichberger, R. Fornika, W. Leitner, *J. Am. Chem. Soc.*, 1997, **119**, 4432–4443;
- [11] A. Uhe, M. Hölscher, W. Leitner, *Chem. Eur. J.* 2012, **18**, 170–177.
- [12] The synthesis, characterization and X-ray crystal structure of *fac-I* will be reported elsewhere: C. Conifer, A. Uhe, S. Stoychev, J. Wülbern, C. Lehmann, J. Rust, M. Hölscher, W. Leitner, manuscript in preparation.
- [13] Gaussian 09, Revision C.01. The full reference can be found in the Supporting Information.
- [14] Y. Zhao, D. G. Truhlar, *J. Chem. Phys.* 2006, **125**:194101.
- [15] F. Weigend, R. Ahlrichs, *Phys. Chem. Chem. Phys.*, 2005, **7**, 3297–3305.
- [16] a) D. Andrae, U. Häußermann, M. Dolg, H. Stoll, H. Preuss, *Theor. Chim. Acta.*, 1990, **77**, 123–141; b) K. A. Peterson, D. Figgen, E. Goll, H. Stoll, M. Dolg, *J. Chem. Phys.*, 2003, **119**, 11113–11123.
- [17] a) B. I. Dunlap, *J. Chem. Phys.*, 1983, **78**, 3140–3142; b) B. Dunlap, *J. Mol. Struct.: THEOCHEM*, 2000, **529**, 37–40.
- [18] J. Tomasi, B. Mennucci, R. Cammi, *Chem. Rev.*, 2005, **105**, 2999–3093.
- [19] a) R. L. Martin, P. J. Hay, L. R. Pratt, *J. Phys. Chem. A*, 1998, **102**, 3565–3573; b) N. Sieffert, M. Bühl, *Inorg. Chem.*, 2009, **48**, 4622–4624.
- [20] a) W. Leitner, *Angew. Chem.*, 1995, **107**, 2391–2405; *Angew. Chem. Int. Ed. Engl.*, 1995, **34**, 2207–2221; b) P. G. Jessop, in *Handbook of Homogeneous Hydrogenation* (Eds.: J. G. De Vries, C. J. Elsevier), Wiley-VCH, Weinheim, 2007, pp. 489–511; c) C. Federsel, R. Jackstell, M. Beller, *Angew. Chem.*, 2010, **122**, 6392–6395; *Angew. Chem. Int. Ed.*, 2010, **49**, 6254–6257.
- [21] a) F. Hutschka, A. Dedieu, *J. Chem. Soc. Dalton Trans.*, 1997, 1899–1902; b) Y. Musashi, S. Sakaki, *J. Am. Chem. Soc.*, 2000, **122**, 3867–3877; c) Y. Musashi, S. Sakaki, *J. Am. Chem. Soc.*, 2002, **124**, 7588–7603; d) Y. Ohnishi, T. Matsunaga, Y. Nakao, H. Sato, S. Sakaki, *J. Am. Chem. Soc.*, 2005, **127**, 4021–4032; e) K. Huang, J. H. Han, C. B. Musgrave, E. Fujita, *Organometallics*, 2007, **26**, 508–513; f) A. Urakawa, F. Jutz, G. Laurenczy, A. Baiker, *Chem. Eur. J.*, 2007, **13**, 3886–3899; g) A. Urakawa, M. Iannuzzi, J. Hutter, A. Baiker, *Chem. Eur. J.*, 2007, **13**, 6828–6840; h) A. D. Getty, C.-C. Tai, J. C. Linehan, P. G. Jessop, M. M. Olmstead, A. L. Rheingold, *Organometallics*, 2009, **28**, 5466–5477.
- [22] a) M. H. G. Prechtel, M. Hölscher, Y. Ben-David, N. Theyssen, R. Loschen, D. Milstein, W. Leitner, *Angew. Chem.*, 2007, **119**, 2319–2322; *Angew. Chem. Int. Ed.*, 2007, **46**, 2269–2272; b) M. H. G. Prechtel, M. Hölscher, Y. Ben-David, N. Theyssen, D. Milstein, W. Leitner, *Eur. J. Inorg. Chem.*, 2008, 3493–3500.
- [23] Tunneling corrections to the σ -bond-metathesis type hydrogen transfer step in *fac*- and *mer-I-TS3-4* were applied using the method described by Skodje and Truhlar^[24], but only led to a negligible lowering of the transition state's height by 1.1 and 0.4 kcal/mol in *mer-I-TS3-4* and *fac-I-TS3-4*, respectively.
- [24] R. T. Skodje and D. G. Truhlar, *J. Phys. Chem.*, 1981, **85**, 624.
- [25] a) S. Kozuch, S. Shaik, *J. Am. Chem. Soc.*, 2006, **128**, 3355–3365; S. Kozuch, S. Shaik, *J. Phys. Chem. A*, 2008, **112**, 6032–6041; b) A. Uhe, S. Kozuch, S. Shaik, *J. Comput. Chem.*, 2011, **32**, 978–985.